ACI STRUCTURAL JOURNAL TECHNICAL PAPER

Title no. 100-S21

# Moment Transfer at Interior Slab-Column Connections

by Scott D. B. Alexander and Sidney H. Simmonds

*Under the American design standard, ACI 318, the strength of slab-column connections is assessed using an interaction equation that includes contributions from both shear and unbalanced moment. Based on a reexamination of tests reported by Hanson and Hanson, rhr unbalanced moment at interior connections is shown to contribute far less to transverse shear than is assumed in design. A simple limit analysis is presented. This analysis is more consistent with observed behavior and accepted material limits and better predicts the test results.*

**Keywords:** column; reinforced concrete; slab.

## BACKGROUND

In the vicinity of a column support. a two-way reinforced concrete plate must carry transverse shear resulting from gravity load. In addition, there may bc a net nioment $M_{unb}$, traditionally called an unbalanced moment. to be transferred between the slab and the column.

For design, ACI 318' limits the calculated maximum stress on a critical section located *di2* from the face of the support. Both the vertical shear and a fraction of the unbalanced moment are assumed to contribute to shear stresses on the critical section. A linear distribution of transverse shear stress is assumed to act on the critical section, with the magnitude oí the shear stress $v$ at any point on the critical section is given hy

$$\gamma_v \cdot M_{unb} \cdot e$$

In **Eq. (1)**, V is the net shear at the centroid of the critical section. $b_0$ is the perimeter of the critical section. $d$ is the average flexural depth oíthe slab, and $e$ is the distance between a point on die critical section and its centroid. The term $\gamma_v$, generally about 0.4 for interior connections, is the fraction of the unbalanced moment assumed to be carried by shear stresses on the critical section and J is a property of the critical section. The nominal limiting value of the stress $v_c$ on the critical section is $0.33\sqrt{f_c'}$ where $f_c'$ is in units of MPa.

The contention of this paper is that unbalanced moment contributes far less tu transverse shear than is implied by Eq. (1). An unbalanced moment generates very high flexural forces in the vicinity ofthe column within the plane of the slab. The argument is based on a reexamination of the tests reported by Hanson and Hanson.[2]

A reexamination of these tests is appropriate for four reasons. First. the specimens. tested under combinations of low net shear and high unbalanced moment. were described as having failed in shear. Second, they are well documented and have well-defined statics, permitting an alternative analysis. Third. the loading geometry reasonably approximates conditions in a prototype slab under lateral load. Finally. the tests are historically significant as they were used to justify the current design assumption that approximately 40% of the unbalanced moment is carried by shear.

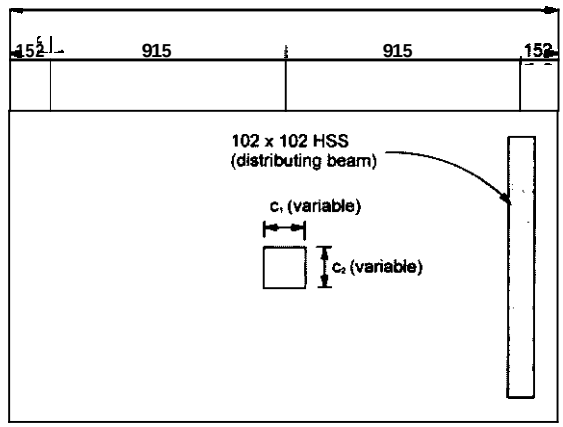


*Fig. 1—Specimen geometry.*

### Tests by Hanson and Hanson[2]

Hanson and Hanson report tests on 16 interior slab-column connections and one edge slab-column connection. Of the interior specimens, three failed in bending and six had perforations immediately adjacent to the column. This discussion will be limited to the remaining seven interior connections without slab perforations that are reported to have failed in shear.

All slabs were 76 mm (3 in.) thick and reinforced with No. 3 bars ($A_{bar}$ = 71 mm$^2$) at 76 mm (3 in.) on center each way top and bottom. The clear cover was 9.5 nun (0.375 in.), giving an average flexural depth of 57 mm (2.25 in.). The outer bars for both the top and bottom mats were placed parallel to the long dimension of the slab.

Figure I shows a plan view of the specimens while Fig. 2 shows the loading arrangement. The support at the top of the column produced compression in the column that was proportional to the applied moment. Details and test results for these specimens are given in Table 1. The loads $P_1$ and $P_2$ are based on satisfying vertical and rotational equilibrium (Eq. (2) and (3)) and assuming a specimen self-weight of 4.46 kN (I .0 kips).

$$V = P_1 - P_2 + 4.46 \text{ kN} \quad (2)$$

$$M_{unb} = (P_1 + P_2) \times 0.915 \text{ m} \quad (3)$$

*ACI Structural Journal*, V. 100. No. 2, March-April 2003.
MS No. 01-419 received December 6, 2001. and reviewed under Institute publication policies.  Pertinent discussion will be published in the January-February 2004 *ACI Structural Journal* if received by September 1, 2003.

*ACI member* **Scott D. B. Alexander** *is an associate professor of civil and environmental engineering at the University of Alberta, Edmonton, Alberta, Canada. He is a member of Joint ACI-ASCE Committees 421, Design of Reinforced Concrete Slabs; and 445, Shear and Torsion.*

**Sidney H. Simmonds**, *FACI, is an emeritus professor of civil and environmental engineering at the University of Alberta. He has served as a member of ACI Committees 118, Use of Computers; 120, History of Concrete; 318, Structural Concrete Building Code; 318-F, New Materials, Products, and Ideas; 340, Strength Design Handbook; and Joint ACI-ASCE Committees 334, Shell Design and Construction; and 421, Design of Slabs.*

Additional internal stress resultants can be determined from equilibrium considerations. Figure 3 shows free body diagrams of the two cantilever portions of slab and the column-slab section between them. The moments and shears $M_1$, $M_2$, $V_1$, and $V_2$ are calculated from equilibrium of the cantilever portions of slab and include the self-weight of the slab.

### Internal forces resulting from moment transfer

The moments $M_1$ and $M_2$ are carried entirely by flexure within the slab and can only be the result of couples formed by forces in the plane of the slab. Considering the larger of the two moments, $M_1$, and dividing by the depth of the slab gives a conservative estimate of the magnitude of the horizontal forces forming the couple. For all tests, this estimate of the horizontal force is between 10 and 15 times the magnitude of the transverse shear $V_1$. Figure 4 illustrates graphically the relative magnitudes of these forces on a free body diagram of the column and central portion of slab. It is clear that the transverse shear is relatively insignificant compared to the in-plane forces.

Because the unbalanced moment is the result of an interaction between the slab and the column, a set of forces statically equivalent to those shown in Fig. 4 must frame into the joint itself. This creates a bottleneck for the flexural tension and compression forces. Bars passing through the joint account for only a portion of the total flexural tension force. The remainder is anchored to the column indirectly, principally through compression in the concrete. The compression forces associated with the anchorage of reinforcement must coexist with the flexural compression forces, all of which must ultimately bear on the joint. At the four faces of the joint itself, the column dimensions impose a geometric limit on the width of the compression block.

Figure 5 shows a sketch of the crack pattern reported in Hanson and Hanson[2] for Specimen A12. Similar crack patterns were reported for all specimens with either Type I or Type III loading. This pattern suggests the strut-and-tie model in Fig. 6, which illustrates the forces associated with reinforcing bars passing outside the joint.

In Fig. 6, dashed lines indicate compression struts and solid lines indicate tension ties. Each top bar is linked to a flexural

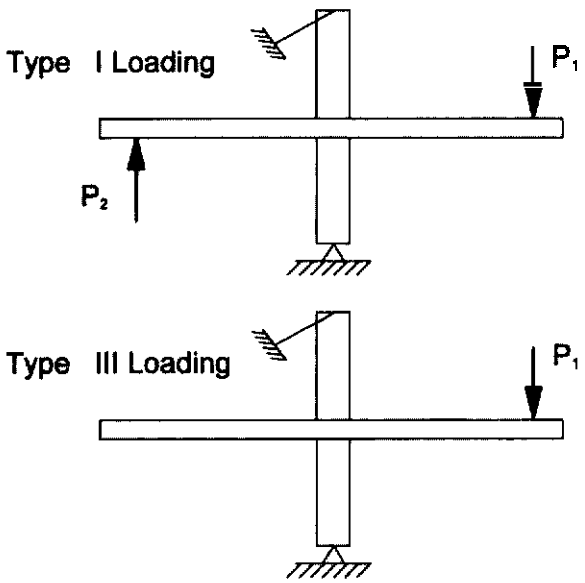


*Fig. 2—Loading arrangement.*

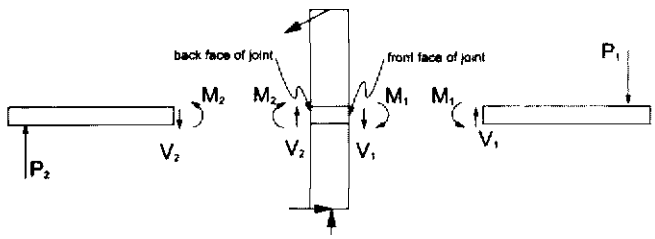


*Fig. 3—Free body diagrams.*

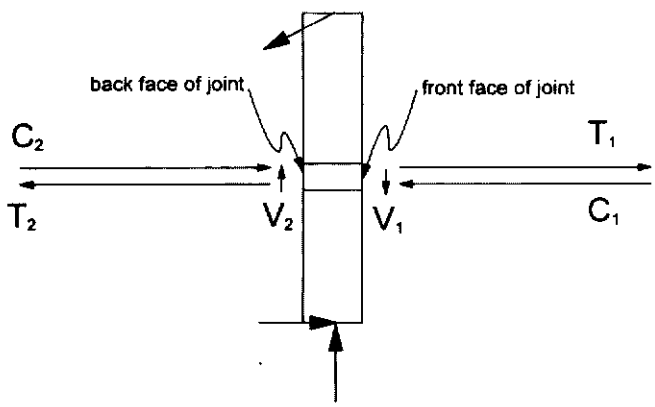


*Fig. 4—In-plane forces.*

**Table 1—Selected specimen measurements and test results**

| | | As reported in Hanson and Hanson (1968) | | | | | | Calculated quantities | | | | | |
|---|---|---|---|---|---|---|---|---|---|---|---|---|---|
| Mark | Type | $f'_c$, MPa | $f_y$, MPa | $c_1$, mm | $c_2$, mm | $V$, kN | $M_{unb}$, kN · m | $P_1$, kN | $P_2$, kN | $M_1$, kN · m | $M_2$, kN · m | $V_1$, kN | $V_2$, kN |
| A1 | I | 30.3 | 366 | 152 | 152 | 5.75 | 22.4 | 12.9 | 11.6 | 11.8 | 8.6 | 15.0 | 9.5 |
| A2 | I | 31.4 | 377 | 152 | 152 | 4.81 | 24.3 | 13.5 | 13.1 | 12.3 | 9.9 | 15.6 | 11.0 |
| B7 | I | 33.0 | 355 | 305 | 152 | 4.90 | 35.8 | 19.8 | 19.3 | 16.0 | 13.7 | 21.7 | 17.4 |
| C8 | I | 32.9 | 412 | 152 | 305 | 5.62 | 31.5 | 17.8 | 16.6 | 15.9 | 12.8 | 19.9 | 14.5 |
| A12 | III | 33.3 | 373 | 152 | 152 | 26.92 | 20.5 | 22.5 | 0 | 19.9 | −1.1 | 24.5 | −2.1 |
| B16 | III | 30.5 | 341 | 305 | 152 | 34.45 | 27.4 | 30.0 | 0 | 23.7 | −1.0 | 31.9 | −2.0 |
| C17 | III | 36.1 | 342 | 152 | 305 | 31.56 | 24.8 | 27.1 | 0 | 23.7 | −1.1 | 29.2 | −2.1 |

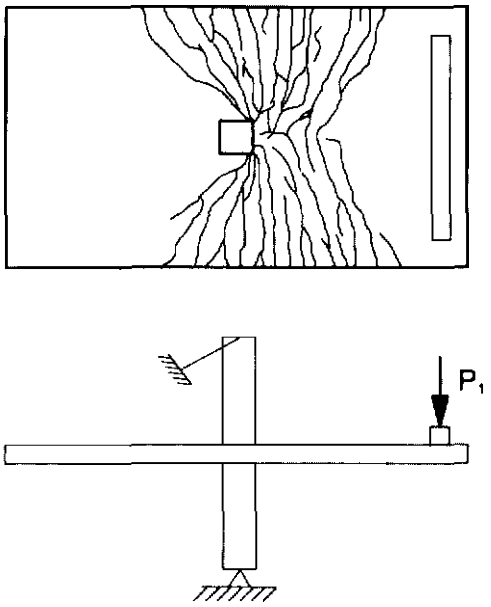


*Fig. 5—Crack pattern—Specimen A12.*

conipression strut bearing on the lower half of the front or side faces of the joint. Top bars passing outside the column are anchored to the backside **of** the column by means of compression struts within the plane **of** the top reinforcement. Anchoring tie forces are providrd by top reinforcement parallel to the front and back faces of the joint. For specimens with Type **I** loading, the bottom bars are engaged in tension, generating an arrangement of struts and ties similar to that associated with the top bars.

The shears $V_1$ and $V_2$ (Fig. **4)** are the vertical components of the flexural conipression struts (Fig. **6).** Because flexural forces are over 10 times greater than the shear forces, the flexural compression struts at the face of the joint are very nearly horizontal (within about five degrees). The total compression framing into the front and side faces of the joint is the sum of the flexural struts and the anchoring struts.

## Limit analysis

The objective of this limit analysis is to provide an estimate **of** the capacity of a slab-column connection to transfer moment as governed by the forces acting within the slab. Forces within the joint itself are nut examined. Reinforcing steel is assumed to act in either tension or compression and is limited to its yield force. Concrete compression stresses are limited to values commonly assumed in flexural design. Concrete tensile stresses and dowel forces are neglected.

The total unbalanced moment $M_{unb}$ is expressed as the sum of two parts. The transverse shears $V_1$ and $V_2$ are eccentric to the center of the column and they are responsible for a portion $M_{shear}$ of the unbalanced moment. The remainder of the unbalanced moment $M_{flex}$ is the vector sum **of** $M_1$ and $M_2$.

Taking the forces shown in Fig. 3 as positive. $M_{shear}$ is given by

$$M_{shear} = (V_1 + V_2) \times \frac{c_1}{2}$$

The ratio of $M_{shear}$ to $M_{unb}$ is fixed by the loading arrangement and the column dimension $c_1$. For the tests by Hanson and Hanson, $M_{shear}$ accounts for 8.3% of $M_{unb}$ where $c_1$ is 152 mm,

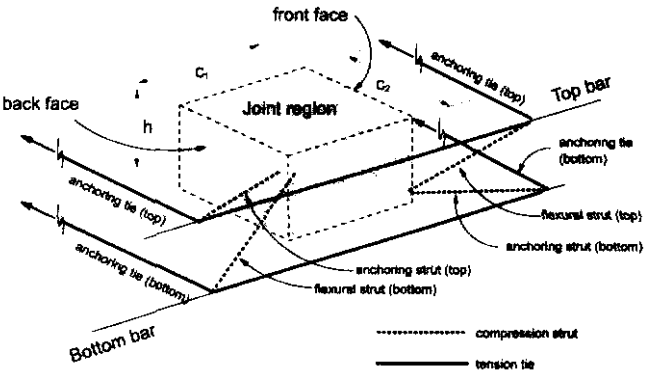


***Fig. 6—Strut-and-tie model for slab reinforcement outside of joint.***

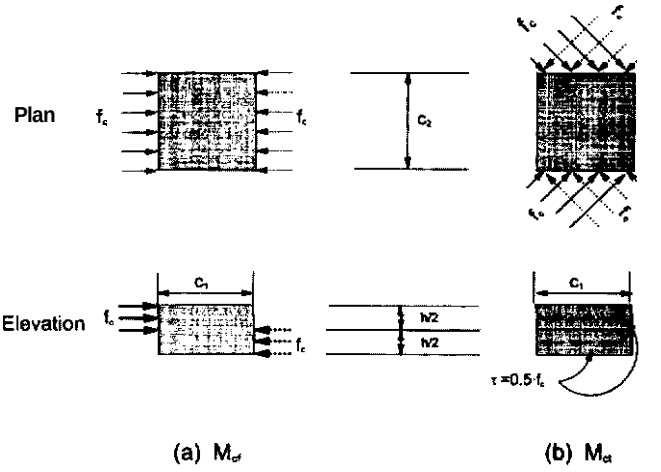


*Fig. 7—Components of moment carried by concrete at joint.*

and **16.7%** of $M_{unb}$ where $c_1$ is **305** mm. It follows that the corresponding values for flexural moment $M_{flex}$ account for 91.7% and 83.3% of the unbalanced moment, respectively. It is the capacity of the specimens to transmit this flexural moment that determines failure.

The moments $M_1$ and $M_2$ produce flexural forces that frame into the joint. These forces are limited by either compression rupture of the concrete at the face of the joint or by yielding of the flexural reinforcement.

$M_{flex}$ is divided into three parts, $M_{cf}$, $M_{ct}$, and $M_s$. $M_s$ is the flexural moment that can be attributed to the reinforcing steel framing into the joint itself. $M_{cf}$ and $M_{ct}$, illustrated in Fig. 7. are moments transferred from the slab to the slab-column joint by way of uniaxial compression stresses in the concrete acting in the plane of the slab. $M_{cf}$ is formed by opposing compression forces on the front and hack faces of the slab-column joint. $M_{ct}$ is a torsional moment transferred on the side faces of the slab-column joint.

To estimate $M_{cf}$, a uniaxial stress $f_c$ is assumed to bear on the faces of the slab-column joint. On the front and back faces, opposing normal stresses are assumed to act over half the depth of the slab. as shown in Fig. 7(a). The half depth of the slab is chosen to maximize $M_{cf}$.

$$M_{cf} = f_c \times c_2 \times \left(\frac{h}{2}\right)^2 \quad (5)$$

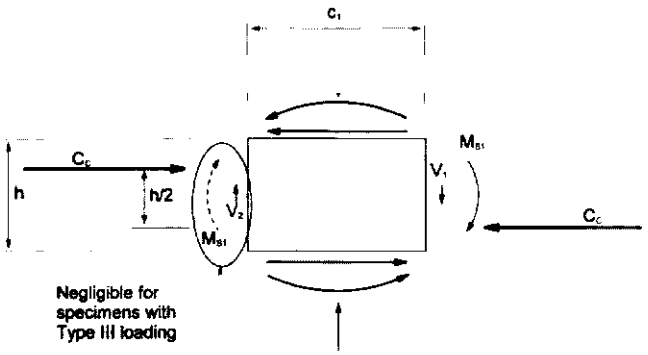


*Fig. 8—Net forces at joint.*

For the torsional moment $M_{cf}$, two uniaxial stress blocks load each side face. To maximize the torsional moment. each uniaxial stress block is assumed to act over half the depth of the slab and to meet the face of the slab-column joint at 45 degrees, as illustrated in the plan view of Fig. 7(b). The uniaxial stress off, at an angle of 45 degrees produces a compression stress of $0.5f_c$ normal to the side face and a shear stress of $0.5f_c$ acting on the side face. Only the shear stress component is shown in the elevation view of Fig. 7(b) because it is only the shear component that transfers moment to the joint.

$$M_{cf} = 2 \times \frac{2}{3} \times c_1 \times \left(\frac{h}{2}\right)^2 \quad (6)$$

It is convenient to add the moments $M_{cf}$ and $M_{cl}$ to produce the total moment carried by concrete compression stresses acting parallel to the plane of the slab $M_c$.

$$M_c = M_{cf} + M_{cl} = f_c(c_1 + c_2)\left(\frac{h}{2}\right)$$

Equation (7) applies to square or rectangular columns. It can be shown that for the case of a round column of radius $R$, the corresponding expression for $M_c$ is

$$M_{c,round} = f_c(\pi R)\left(\frac{h}{2}\right)^2 \quad (8)$$

Reinforcing steel framing directly into the joint contributes to the unbalanced moment as either tension or compression reinforcement and by transferring horizontal dowel forces on the side faces of the joint. Because the expressions for $M_c$ neat the joint faces as if they are solid concrete. some allowance should be made for the concrete displaced by compression reinforcement. Ignoring dowel forces, a simple estimate for the moment carried by steel on one face of the connection is

$$M_{s1} = A_{s1} \times (f_y - f_c) \times h' \quad (9)$$

where $A_{s1}$ is the area of compression reinforcement framing into the joint face and h' is the distance between the centroid of the top and bottom bars. For the specimens with Type III loading, $M_s$ is taken equal to $M_{s1}$. For the specimens with Type I loading, both the upper and lower mats of reinforcement are engaged in tension and there is the potential to generate $M_{s1}$ on both the front and back faces of the joint. This requires the reinforcing bars to go from tension to compression yield within the length of the slab-column joint. a circumstance that is considered plausible given the highly confined state of the joint. As a result, $M_s$ is taken as twice $M_{s1}$ for specimens with Type I loading.

It is useful to replace $M_c$ with a couple formed by two compression forces labeled $C_c$ as shown in Fig. 8. For specimens with rectangular columns. the magnitude of $C_c$ is given hy

$$C_c = \frac{2 \cdot M_c}{h} = f_c(c_1 + c_2)\left(\frac{h}{2}\right) \quad (10)$$

Based on the rectangular flexural stress block parameters described in the ACI 318[1] standard, $f_c = 0.85f_c'$ is a reasonable limit if compression failure of the concrete governs the magnitude of $C_c$.. Alternaiively. considering u free body diagram of one of the slab cantilevers, horizontal cqiiilihrium requires that $C_c$ be inatched hy an equal tension in the reinforcing steel. Therefore, the magnitude of $C_c$ may be limited by the available tension reinforcement.

$$C_c = 0.85f_c'(c_1 + c_2)\left(\frac{h}{2}\right) \le N_{bars} \times A_{bar} \times f_y \quad (11)$$

For specimens with Type I loading. with both top and bottom reinforcement engaged in tension, the numher of reinforcing bars potentially available to equilihratc $C_c$ is 32 less the numher of top and bottom bars passing through the column. Note that the tlexural contribution of bars passing throiigh the column is accounted for in the calculation of $M_s$. For specimens with Type III loading. only the top reinforcement is engaged in tension. limiting the total nomher of available hars to 16 less the number of top bars passing through the column. Table 2 lists values for $C_c$ consistent with the two limits expressed in Eq. (9). Two specimens, B16 and C17, are governed by yielding of the reinforcenient.

A revised expression for $M_c$ that accounts for the potential limit imposed by slab reinforcement is

$$M = C \times \left| h - \frac{\quad}{85(c_1 + c_2)f_c'} \right.$$

Table 2 presents predicted values of unbalanced moment at failure and compares these to test results. For relerence. predictions based on ACI 318[1] are also provided.

## DISCUSSION

The results listed in Table 2 show that the tests hy Hanson and Hanson are well predicted by the limit analysis described in this paper. The analysis tends to underestimate the capacity of the connection. This is somewhat surprising. Given the aggressive assumptions with regard to concrete rupture and loading geometry that were used in calculating $M_c$, it is difficult to imagine how the concrete might contribute further to moment transfer. It is possible that biaxial and triaxial loading effects increased the apparent strength of the concrete at the face of the joint. Apart from some additional strength that may he attrihuted to horizontal dowel forces on the side faces of the joint. ignored in the analysis. all potential

**Table 2—Results of analyses**

| | | Limit analyses | | | | | | ACI 318 | |
|---|---|---|---|---|---|---|---|---|---|
| Mark | Type | $C_c$, kN (concrete limit) | $C_s$, kN (steel limit) | $M_c$, kN · m | $M_s$, kN · m | $M_{pred}$, kN · m | Test/pred. | $V_c$, MPa | Test/pred. |
| A1 | I | 299 | 731 | 11.41 | 4.62 | 17.5 | 1.28 | 2.75 | 1.51 |
| A2 | I | 310 | 751 | 11.80 | 4.75 | 18.0 | 1.35 | 2.96 | 1.60 |
| B7 | I | 489 | 709 | 18.63 | 4.44 | 27.7 | 1.29 | 2.50 | 1.32 |
| C8 | I | 487 | 704 | 18.55 | 10.42 | 31.6 | 1.00 | 2.11 | 1.11 |
| A12 | III | 329 | 372 | 12.52 | 2.34 | 16.2 | 1.27 | 2.97 | 1.56 |
| B16 | III | 451 | 340 | 16.15 | 2.14 | 22.0 | 1.25 | 2.38 | 1.31 |
| C17 | III | 534 | 292 | 16.18 | 4.23 | 22.3 | 1.11 | 2.08 | 1.05 |
| Mean | | | | | | | 1.22 | | 1.35 |
| Standard deviation | | | | | | | 0.123 | | 0.217 |
| Coefficient of variation, % | | | | | | | 10.1 | | 16.1 |

moment transfer capacity that can he attributed to slab reinforcement in the joint has been included.

The lowest test to predicted ratios are for Specimens C8 and C17. These specimens have rectangular columns with $c_2$ greater than $c_1$, making the contribution of dowel forces on the side faces proportionately less significant. The larger column width reduces the clamping effect of the axial compression in ihe column. In the case of Specimen C8, this combined with the smaller value of $c_1$, the highest reported yield strength. and Type I loading would make the bond stresses needed to justify the calculation of $M_s$ unlikely. Recall that in calculating $M_s$ for Type I specimens it was assumed that reinforcement could pass from tension yield to compression yield within the length $c_1$.

Although listed as punching failures, this analysis suggests Specimens B16 and C17 were limited by the available reinforcement. Hanson and Hanson also report that these specimens exceeded their ultimate flexural capacities before failing in shear. An alternate explanation is that the compressive stresses at the face of the joint became critical at about the same moment that the slab flexural reinforcement reached yield. This is analogous to a beam with close to balanced reinforcement. failing in tlexure hut with limited ductility.

While the results obtained using ACI 318 listed in Table 2 are all safe, their higher coefficient of variation indicates less reliability than those obtained using the limit analysis. The procedure of increasing the transverse shear stress with a fictional shear stress calculated from unbalanced moment does not agree with test results as well as a simple limit analysis that uses straightforward failure criteria. In particular, the computational complexity of the terms J and $\gamma_v$ used in Eq. (1) does not seem justified.

This does not mean that the code procedure is inappropriate for design. So long as its application is confined to the critical section for which it was empirically tuned. the code procedure may provide a reasonable metric for the severity of loading at a slab-column connection. If there is any danger, it lies in accepting as sound the mechanics upon which the code procedure is hascd and applying these mechanics at critical sections more distant from the column.

The analysis shows that while a fraction of the unbalanced moment can be attributed to transverse shear, this fraction was much smaller than $\gamma_v$ for the tests reported in Hanson and Hanson. In a prototype slab-column system. the fraction of unbalanced nioment carried by shear would be smaller still. roughly equal to the ratio of the column dimension $c_1$ to the sum of the spans on either side of the connection.

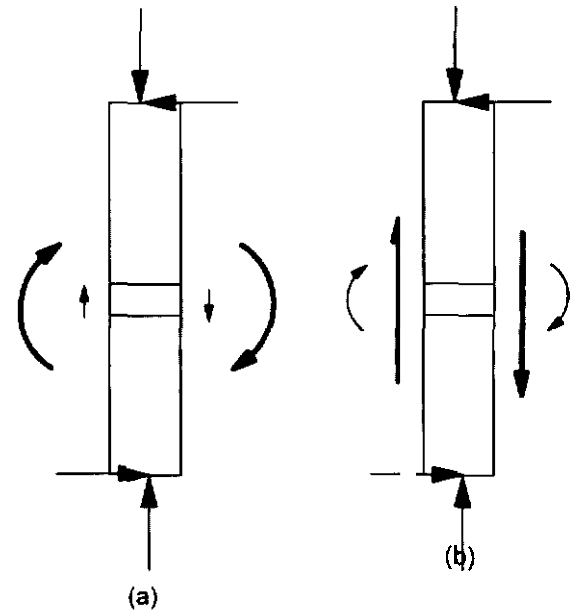


*Fig. 9—Statically equivalent load cases.*

in a laboratory test, it is possible to increase the fraction of unbalanced moment attributable to transverse shear. For example, consider an isolated connection specimen with a small portion of attached slab that extends out from the column to roughly the first point of radial inflection. By providing simple supports on the perimeter of the slab and loading the column so as to produce a high ratio of moment to shear, one might achieve a value of $\gamma_v$ consistent with that estimated by code. The proximity of the slab support reactions to the column greatly reduces the eccentricity of slab load slab and increases the fraction of unbalanced moment carried by shear; however, such a load case would be atypical for a prototype slab-column system,

Figure 9 illustrates two possible combinations of shear and moment to transfer a given unbalanced moment at a slab-column connection. in Fig. 9(a), the unbalanced moment is mainly the result of the vector sum of the slab bending moments on the front and back faces of the column. The fraction of moment transferred by shear is small. Such a connection is typical of those tested by Hanson and Hanson. A prototype structure would also behave this way. In Fig. 9(b), the connection transfers the same total unbalanced moment; however, in this case it is largely the result of significant transverse shears. This behavior would be consistent with an

isolated connection specimen with a relatively small slab supported on all sides. Although these two cases are clearly distinct, they are treated identically by the code.

## CONCLUSIONS

Despite being described as shear failures, the seven specimens tested reponed by Hanson and Hanson[2] and analyzed herein were not critically loaded in transverse shear. Instead, they failed by rupture of concrete in compression, much like over-reinforced beams. At a slab-column connection, such a failure would be indistinguishable from a punching failure.

An equilibrium analysis shows that the total unbalanced moment should be considered in two parts. The first is attributed to transverse shear and the second to flexural forces in the plane of the slab. The relative magnitude of these two components is a function of the span and loading geometry and the column dimension $c_1$.

Although the predictions of the ACI Code are safe, a simple limit analysis provides a substantially better explanation of the ultimate behavior of these tests. The calculation of $\gamma_v$ and $J_c$ is an unnecessary complication and does not reflect the mechanics of load transfer at a slab-column connection. While the code model may provide a reasonable measure of the severity of loading at a slab-column connection, the assumed internal stress distribution the model is based on is fundamentally wrong. Extrapolating the code model to critical sections located beyond $d/2$ from the support is not justified.

Unbalanced moment produces substantial in-plane flexural forces that are ignored in the code approach. These forces are far more significant than the transverse shears and account for a substantially greater fraction of the total unbalanced moment.

## NOTATION

$b_0$ = perimeter of critical section
$c_1, c_2$ = dimensions of column
$d$ = flexural depth of slab
$e$ = distance between extreme point on and centroid of critical section
$f_c$ = limiting uniaxial concrete stress in flexure
$f_c'$ = concrete cylinder strength
$h$ = thickness of slab
$h'$ = distance between slab tension and compression reinforcement
$J_c$ = section property of critical section
$M_c$ = total moment from concrete stresses within plane of slab; Eq. (7)
$M_{cf}$ = moment from concrete compression bearing on front and back faces of a joint; Eq. (5)
$M_{cs}$ = moment from shear on side faces of joint; Eq. (6)
$M_s$ = total moment carried by slab reinforcement passing through joint
$M_{sf}$ = moment at one face of joint carried by slab reinforcement passing through joint; Eq. (9)
$M_{shear}$ = moment at centroid of column from slab shears $V_1$ and $V_2$; Eq. (4)
$M_{unb}$ = net moment transferred from slab to column (unbalanced moment) at failure
$M_1, M_2$ = total supporting moments for slab cantilevers defined in Fig. 3
$P_1, P_2$ = loads applied to slab defined in Fig. 2
$V$ = net shear transferred from slab to column at failure
$V_1, V_2$ = total supporting shears for slab cantilevers defined in Fig. 3
$v_c$ = maximum shear stress on critical section as calculated by Eq. (1)
$\gamma_v$ = fraction of $M_{unb}$ assumed to be transferred by shear

## REFERENCES


1. ACI Committee 318, "Building Code Requirements for Structural Concrete (ACI 318-02) and Commentary (318R-02)," American Concrete Institute, Farmington Hills, Mich., 2002, 443 pp.

2. Hanson, N. W., and Hanson, J. M., "Shear and Moment Transfer Between Concrete Slabs and Columns," *Journal of the PCA Research and Development Laboratories*, V. 10, No. 1, Jan. 1968, pp. 2-16.